Anal. Chem. **2010,** *82,* 9636–9643

Complete Physicochemical Characterization of DNA/Chitosan Complexes by Multiple Detection Using Asymmetrical Flow Field-Flow Fractionation

Pei Lian Ma,[†,‡] Michael D. Buschmann,[†,§] and Françoise M. Winnik*,[||]

Department of Chemical Engineering and Institute of Biomedical Engineering, Ecole Polytechnique de Montréal, P. O. 6079 Succursale Centre-Ville, Montreal, Quebec, Canada H3C 3A7, and Department of Chemistry and Faculty of Pharmacy, Université de Montréal, P. O. 6128 Succursale Centre-Ville, Montréal, Québec, Canada H3C 3J7

Asymmetrical flow field-flow fractionation (AF4) coupled with UV−vis spectrophotometry, multiangle light scattering (MALS), and dynamic light scattering (DLS) detection was used to analyze dispersions of DNA/rhodamine B labeled chitosan (Ch-rho) complexes frequently used as gene delivery vectors. The method yielded, in a single experiment, important characteristics of the complexes, such as their hydrodynamic radius, size distribution, conformation, composition, and the amount of free Ch-rho in the dispersions. Samples for analysis were obtained by varying experimental parameters known to influence the transfection efficiency of DNA/chitosan complexes, including the DNA concentration at mixing (82−164 μg/mL), the ratio of chitosan amino groups to DNA phosphate groups (3 ≤ N/P ratio ≤ 15), the chitosan molecular weight (10−76 kDa), and its degree of deacetylation. In all preparations, DNA/Ch-rho complexes had hydrodynamic radii ranging from 15 to 160 nm. Both the DNA concentration and the Ch-rho molecular weight influence the size distribution of the complexes: a greater fraction of large particles was detected in dispersions prepared with the most concentrated DNA solution or the Ch-rho of highest molar mass. All dispersions contained free Ch-rho in solution. The free Ch-rho content ranged from 53 to 92% of the total Ch-rho concentration in dispersions prepared with N/P ratios from 3 to 15, respectively, implying that the N/P ratio of the complexes ranged from 1.3 to 1.6 in all samples. The accuracy of the free Ch-rho determination by AF4/UV−vis/MALS+DLS was confirmed by an independent method involving (1) ultracentrifugation of the dispersions prepared with unlabeled chitosan and (2) analysis of the supernatant by the Orange II dye depletion method. This study demonstrates the ability of AF4/UV−vis/MALS+DLS to provide a complete physicochemical characterization of DNA/polycation complexes used in nonviral gene delivery.

Cationic polymers have been extensively investigated as vectors for gene delivery due to their low immunogenicity, their enhanced safety compared to their viral counterparts, and the ease of their preparation. Cationic polymers condense DNA through electrostatic interactions to form nanoparticles that can be internalized by cells. It has been observed that for efficient in vitro and in vivo transfection to occur, the DNA/polycation complexes should be prepared by mixing DNA with an excess of polycation, such that the molar ratio of polycation protonable amino groups to DNA phosphate groups, known as the N/P ratio, is about 3 or higher.[1−4] These conditions generate positively charged nanoparticles which resist aggregation as a consequence of repulsive electrostatic forces. Typically, not all of the polycation binds to DNA. The excess polycation, which is dissolved in the aqueous medium, appears to play a critical role in the transfection process, possibly by triggering the endosomal escape of the complexes through the proton sponge effect.[1,5−7] According to this hypothesis, polycations act as buffers in the endosome by absorbing a large amount of protons that generate an influx of chloride ions to maintain electroneutrality.[8,9] The resulting increase of the osmotic pressure causes the rupture of the endosomes and the release of the complexes in the cytoplasm. Calculations based on the Poisson−Boltzmann theory have predicted that the endosome must contain a sufficiently large amount of free polycation for the proton sponge effect to take place.[10] The DNA/polycation complexes alone are unable to induce the rupture of the endosomal membrane. The proton sponge hypothesis has been invoked

* To whom correspondence should be addressed: Phone: 1-514-340-5179. Fax: 1-514-340-5292. E-mail: francoise.winnik@umontreal.ca.

[†] Ecole Polytechnique de Montréal.

[‡] E-mail: pei-lian.ma@polymtl.ca.

[§] E-mail: michael.buschmann@polymtl.ca.

[||] Université de Montréal.

(1) Boeckle, S.; von Gersdorff, K.; van der Piepen, S.; Culmsee, C.; Wagner, E.; Ogris, M. *J. Gene Med.* **2004**, *6*, 1102–1111.

(2) Koping-Hoggard, M.; Varum, K. M.; Issa, M.; Danielsen, S.; Christensen, B. E.; Stokke, B. T.; Artursson, P. *Gene Ther.* **2004**, *11*, 1441–1452.

(3) Jean, M.; Smaoui, F.; Lavertu, M.; Methot, S.; Bouhdoud, L.; Buschmann, M. D.; Merzouki, A. *Gene Ther.* **2009**, *16*, 1097–1110.

(4) Strand, S. P.; Lelu, S.; Reitan, N. K.; de Lange Davies, C.; Artursson, P.; Varum, K. M. *Biomaterials* **2010**, *31*, 975–987.

(5) Clamme, J. P.; Azoulay, J.; Mely, Y. *Biophys. J.* **2003**, *84*, 1960–1968.

(6) Saul, J. M.; Wang, C. H. K.; Ng, C. P.; Pun, S. H. *Adv. Mater.* **2008**, *20*, 19–25.

(7) Ma, P. L.; Buschmann, M. D.; Winnik, F. M. *Biomacromolecules* **2010**, *11*, 549–554.

(8) Boussif, O.; Lezoualc'h, F.; Zanta, M. A.; Mergny, M. D.; Scherman, D.; Demeneix, B.; Behr, J. P. *Proc. Natl. Acad. Sci. U.S.A.* **1995**, *92*, 7297–7301.

(9) Behr, J.-P. *Chimia* **1997**, *51*, 34–36.

(10) Yang, S.; May, S. *J. Chem. Phys.* **2008**, *129*, 185105–185109.

10.1021/ac100711j
Published on Web 11/05/2010

frequently, but it remains a somewhat controversial issue.[11,12] To clarify issues related to the role of the free polycation and in view of the inherent toxicity of several polycations used for transfection,[13] it is important to determine accurately and reliably the concentration of free polycation in dispersions and the N/P ratio of DNA/polycation complexes themselves, in particular in cases where high nominal N/P ratios of the mixing components (between 20 and 60 for DNA formulations[2,4,14,15] and up to 150 for small interfering RNA (siRNA) vectors[16,17]) appear to be effective.

The free components present in gene delivery dispersions are readily detectable by gel electrophoresis coupled with selective staining with ethidium bromide and coomassie blue of the migrating DNA and the polycation, respectively.[18,19] This technique provides qualitative information on the presence of free and bound components in the mixture. Isothermal titration calorimetry (ITC) yields the stoichiometry of binding along with the binding affinity by analyzing thermal events involved in the DNA−polycation interaction.[20] Once electrostatic neutralization is achieved in a titration, the neutral complexes precipitate and the polycation added beyond this point will merely be subjected to dilution without binding to the precipitated complexes. The stepwise addition of the titrant (polycation) to a DNA solution carried out in an ITC measurement is indeed different from the standard one-shot fast mixing of DNA with a large excess of polycation, employed to prepare nonviral gene delivery vehicles. Ultrafiltration[21] and size exclusion chromatography (SEC)[1,6,22] have been used to separate the free polycation from DNA complexes. The concentration of free polycation was determined subsequently by fluorescence or colorimetric assays of the filtrate or the collected fractions, respectively. These methods are not without technical difficulties. For example, ultrafiltration can be hindered by build-up of material on the membrane surface, while common problems encountered in SEC are loss of material, interaction of the complexes with the packing, and column blockages. Analysis of DNA/polycation dispersions by fluorescence correlation spectroscopy (FCS) provides quantitative data on the free polycation content without involving an additional separation step. The free polycation concentration is derived from fits of the autocorrelation data to mathematical models that assume the presence of two species diffusing with different rates.[5,23] Data from different studies have not always be consistent. For instance, depending on the method employed, analysis of dispersions of identical total N/P ratio yielded different values for the amount of free poly(ethyleneimine) (PEI) in DNA/PEI dispersions.[1,5] Data gathered by SEC showed a marked increase of the free PEI concentration with the N/P ratio,[1] while data recovered from FCS analysis displayed no dependence on this parameter.[5] Such discrepancies need to be resolved, preferably by the use of alternative methods. The characterization of the DNA/polycation complexes themselves requires another set of analyses. The size and size distribution of the nanoparticles are obtained usually by dynamic light scattering (DLS), which yields the hydrodynamic radius of the complexes, and via imaging techniques such as transmission electron microscopy (TEM), scanning electron microscopy (SEM), and atomic force microscopy (AFM). The surface charge of the complexes can be approximated from ζ potential measurements. We communicated recently a new method to characterize a DNA/polycation dispersion using asymmetrical flow field−flow fractionation (AF4) coupled with a UV−vis spectrophotometer, multiangle light scattering (MALS), and DLS detectors.[7] The principles of AF4 separation are based on the diffusion properties of the analytes. The method, which has been well-described elsewhere,[24−27] has been used to determine the size and size distributions of colloidal suspensions,[28−30] various delivery systems,[31−37] and polymers.[38−42]

In this study, we applied AF4/UV−vis/MALS+DLS to analyze dispersions of DNA/chitosan complexes obtained following various preparation protocols. Chitosan, a naturally derived cationic polysaccharide, is a versatile, biocompatible, and biodegradable material extensively used in DNA transfection studies and in the emerging field of gene silencing using RNA interference.[14,43] Parameters known to affect the transfection efficiency of DNA/

(11) Funhoff, A. M.; van Nostrum, C. F.; Koning, G. A.; Schuurmans-Nieuwenbroek, N. M. E.; Crommelin, D. J. A.; Hennink, W. E. *Biomacromolecules* **2004**, *5*, 32–39.
(12) Gabrielson, N. P.; Pack, D. W. *Biomacromolecules* **2006**, *7*, 2427–2435.
(13) Godbey, W. T.; Wu, K. K.; Mikos, A. G. *Biomaterials* **2001**, *22*, 471–480.
(14) Strand, S. P.; Issa, M. M.; Christensen, B. E.; Varum, K. M.; Artursson, P. *Biomacromolecules* **2008**, *9*, 3268–3276.
(15) Germershaus, O.; Mao, S.; Sitterberg, J.; Bakowsky, U.; Kissel, T. *J. Controlled Release* **2008**, *125*, 145–154.
(16) Liu, X.; Howard, K. A.; Dong, M.; Andersen, M. O.; Rahbek, U. L.; Johnsen, M. G.; Hansen, O. C.; Besenbacher, F.; Kjems, J. *Biomaterials* **2007**, *28*, 1280–1288.
(17) Howard, K. A.; Paludan, S. R.; Behlke, M. A.; Besenbacher, F.; Deleuran, B.; Kjems, J. *Mol. Ther.* **2008**, *17*, 162–168.
(18) Zhao, X.; Pan, F.; Zhang, Z.; Grant, C.; Ma, Y.; Armes, S. P.; Tang, Y.; Lewis, A. L.; Waigh, T.; Lu, J. R. *Biomacromolecules* **2007**, *8*, 3493–3502.
(19) Zhao, X.; Zhang, Z.; Pan, F.; Waigh, T. A.; Lu, J. R. *Langmuir* **2008**, *24*, 6881–6888.
(20) Ma, P. L.; Lavertu, M.; Winnik, F. M.; Buschmann, M. D. *Biomacromolecules* **2009**, *10*, 1490–1499.
(21) Erbacher, P.; Bettinger, T.; Brion, E.; Coll, J.-L.; Plank, C.; Behr, J.-P.; Remy, J.-S. *J. Drug Targeting* **2004**, *12*, 223–236.
(22) Storkle, D.; Duschner, S.; Heimann, N.; Maskos, M.; Schmidt, M. *Macromolecules* **2007**, *40*, 7998–8006.
(23) Reitan, N. K.; Maurstad, G.; de Lange Davies, C.; Strand, S. P. *Biomacromolecules* **2009**, *10*, 1508–1515.
(24) Wahlund, K. G.; Giddings, J. C. *Anal. Chem.* **1987**, *59*, 1332–1339.
(25) Litzen, A.; Wahlund, K. G. *Anal. Chem.* **1991**, *63*, 1001–1007.
(26) Litzen, A. *Anal. Chem.* **1993**, *65*, 461–470.
(27) Schimpf, M. E., Caldwell, K., Giddings, J. C., Eds. *Field-Flow Fractionation Handbook*; John Wiley & Sons: New York, 2000; p 616.
(28) Lee, S.; Rao, S. P.; Moon, M. H.; Giddings, J. C. *Anal. Chem.* **1996**, *68*, 1545–1549.
(29) Pauck, T.; Colfen, H. *Anal. Chem.* **1998**, *70*, 3886–3891.
(30) Prestel, H.; Niessner, R.; Panne, U. *Anal. Chem.* **2006**, *78*, 6664–6669.
(31) Lee, H.; Williams, S. K. R.; Allison, S. D.; Anchordoquy, T. *J. Anal. Chem.* **2001**, *73*, 837–843.
(32) Fraunhofer, W.; Winter, G.; Coester, C. *Anal. Chem.* **2004**, *76*, 1909–1920.
(33) Yohannes, G.; Pystynen, K.-H.; Riekkola, M.-L.; Wiedmer, S. K. *Anal. Chim. Acta* **2006**, *560*, 50–56.
(34) Jahn, A.; Vreeland, W. N.; DeVoe, D. L.; Locascio, L. E.; Gaitan, M. *Langmuir* **2007**, *23*, 6289–6293.
(35) Augsten, C.; Kiselev, M. A.; Gehrke, R.; Hause, G.; Mäder, K. *J. Pharm. Biomed. Anal.* **2008**, *47*, 95–102.
(36) Smith, M. H.; South, A. B.; Gaulding, J. C.; Lyon, L. A. *Anal. Chem.* **2010**, *82*, 523–530.
(37) Hupfeld, S.; Moen, H. H.; Ausbacher, D.; Haas, H.; Brandl, M. *Chem. Phys. Lipids* **2010**, *163*, 141–147.
(38) Liu, M. K.; Giddings, J. C. *Macromolecules* **1993**, *26*, 3576–3588.
(39) Viebke, C.; Williams, P. A. *Anal. Chem.* **2000**, *72*, 3896–3901.
(40) Andersson, M.; Wittgren, B.; Wahlund, K.-G. *Anal. Chem.* **2001**, *73*, 4852–4861.
(41) Takahashi, R.; Al-Assaf, S.; Williams, P. A.; Kubota, K.; Okamoto, A.; Nishinari, K. *Biomacromolecules* **2003**, *4*, 404–409.
(42) Augsten, C.; Maeder, K. *Int. J. Pharm.* **2008**, *351*, 23–30.
(43) Tiera, M. J.; Qiu, X.-P.; Bechaouch, S.; Shi, Q.; Fernandes, J. C.; Winnik, F. M. *Biomacromolecules* **2006**, *7*, 3151–3156.

Table 1. Molecular Characteristics of the Rhodamine-Labeled Chitosans

DDA (%)	M_n[a] (kDa)	M_w/M_n[a]	level of rhodamine B labeling (mol % rho/NH_2)
72	35	1.3	1.7
80	42	1.4	1.2
80	76	1.6	1.2
92	10	1.3	1.3
92	41	1.4	1.4

[a] By SEC analysis of unlabeled chitosans.

chitosan complexes include the N/P ratio and the DNA concentration at mixing as well as the molecular weight and degree of deacetylation (molar fraction of glucosamine monomers or DDA) of the chitosan.[44−47] We demonstrate here the ability of AF4/UV−vis/MALS+DLS to assess in a single measurement the effects of these key parameters on the size, size distribution, conformation, and composition of the particles and on the free polycation content. The validity of the free polycation concentration determined by AF4/UV−vis/MALS+DLS was examined by comparison with data obtained by ultracentrifugation and subsequent quantitative analysis of the free polycation in the supernatant by the Orange II dye depletion method.

MATERIALS AND METHODS

Materials. The 6.4 kb plasmid EGFPLuc (Clontech Laboratories, Mountain View, CA, USA) was amplified in DH5α bacteria and purified using the Qiagen Plasmid Mega Kit (Mississauga, Canada). A stock solution of this plasmid (0.33 mg/mL) was prepared in deionized water and stored at −20 °C before use. Ultrapure heterogeneously deacetylated chitosans (Ultrasan) with a DDA of 72, 80, and 92% were provided by Biosyntech Inc. (Laval, Quebec, Canada) and were depolymerized according to Lavertu et al.[47] using nitrous acid to achieve specific number-average molecular weight (M_n) of 10, 40, and 76 kDa. The chitosans were labeled with rhodamine B−isothiocyanate (Sigma-Aldrich, product no R1755, St. Louis, MO, USA) as previously reported.[7] Table 1 summarizes the M_n and polydispersity index of chitosans, measured by analytical SEC,[48] the DDA, determined by ^{1}H NMR,[49] and the level of rhodamine B measured by UV−vis spectrophotometry.[7] Orange II was from Sigma-Aldrich (product no. 195235).

Preparation of DNA/Chitosan Complexes. Unlabeled chitosan (Ch) and labeled chitosan (Ch-rho) stock solutions of 5 mg/mL were prepared by dissolving the polymer overnight in deionized water and hydrochloric acid (from 1 M HCl solution, Sigma-Aldrich), to reach an HCl/glucosamine ratio of 1. The Ch or Ch-rho solutions were diluted with deionized water to reach the desired ratio of chitosan amino groups to DNA phosphate groups (N/P ratio) when 100 μL of Ch or Ch-rho are mixed with 100 μL of a DNA solution at a concentration of 82 μg/mL in deionized water. This concentration of DNA solution was used in all preparations, except the experiment aimed at examining the effect of DNA concentration, where a 164 μg/mL DNA solution was used. The mixing was done quickly by up and down pipetting of the dispersions. Samples were allowed to incubate at room temperature 30 min before analysis.

AF4/UV−vis/MALS+DLS System. An asymmetrical flow field−flow fractionation system (AF 2000 MT, Postnova Analytics, Salt Lake City, UT, USA) with a channel thickness of 350 μm fitted with a special regenerated cellulose membrane (10 kDa cutoff, RC amphiphilic, Z-MEM-AQU-631, Postnova Analytics) suitable for analysis of amphiphilic or cationic polymers was used. The AF4 was connected to a UV−vis variable wavelength spectrophotometer (SPD-20A, Postnova Analytics), a multiangle light scattering detector (MALS, Dawn Heleos 8+, Wyatt Technology, Santa Barbara, CA, USA), and a dynamic light scattering (DLS) detector (WyattQELS, Wyatt Technology) which is an add-on unit connected to the 108° angle of the MALS Dawn Heleos 8+ detector. The MALS was equipped with a K5 cell and a GaAs laser operating at 658 nm. MALS and DLS data points were collected at a time interval of 1 and 3 s, respectively. Data collection and analysis were done using the ASTRA software (version 5.3.4.15, Wyatt Technology).

AF4 Separation Conditions. The carrier medium was a prefiltered 50 mM acetic acid/sodium acetate buffer at pH 4.0 with a total ionic strength of 20 mM (adjusted by addition of NaCl). After flow equilibration, the sample was injected with a flow rate of 0.2 mL/min (injection loop volume, 21 μL), followed by a 9 min focusing with a cross-flow rate and a detector flow rate of 1 mL/min each. Following a 1 min transition, a four-step cross-flow rate gradient was initiated for the elution mode. The starting flow rate (1 mL/min) was decreased exponentially first with an exponent factor of 0.4 to 0.4 mL/min within 10 min and then with an exponent factor of 0.8 from 0.4 to 0.15 mL/min within 20 min, and finally it was decreased linearly from 0.15 to 0.05 mL/min within 15 min. The cross-flow rate was then kept constant at 0.05 mL/min for 15 min. The detector flow rate was kept at 1 mL/min throughout. All the flow rates were controlled by the AF2000 Control software (Postnova Analytics). The cross-flow was generated by Kloehn syringe pumps (Postnova Analytics), while the axial and focusing flows were delivered by isocratic pumps (PN1130, Postnova Analytics).

Evaluation of UV−vis, MALS, and DLS Data. The detection of the eluted species was performed sequentially by UV−vis absorbance at a wavelength (λ) of 260 (DNA/Ch-rho nanoparticles) or 556 nm (Ch-rho), MALS, and DLS. The free Ch-rho content was quantified using the AF4/vis fractograms recorded at 556 nm. The integrated areas under the curves of the corresponding peak in the fractograms before and after complexation with DNA were compared. The characteristics of the DNA/Ch-rho nanoparticles were obtained by analysis of the corresponding peak in AF4/UV/MALS+DLS fractograms. For every eluted slice of 1 s, the MALS data in the angular range of 35−90° were

(44) MacLaughlin, F. C.; Mumper, R. J.; Wang, J.; Tagliaferri, J. M.; Gill, I.; Hinchcliffe, M.; Rolland, A. P. *J. Controlled Release* **1998**, *56*, 259–272.
(45) Koping-Hoggard, M.; Tubulekas, I.; Guan, H.; Edwards, K.; Nilsson, M.; Varum, K. M.; Artursson, P. *Gene Ther.* **2001**, *8*, 1108–1121.
(46) Ishii, T.; Okahata, Y.; Sato, T. *Biochim. Biophys. Acta Biomembr.* **2001**, *1514*, 51–64.
(47) Lavertu, M.; Methot, S.; Tran-Khanh, N.; Buschmann, M. D. *Biomaterials* **2006**, *27*, 4815–4824.
(48) Darras, V.; Nelea, M.; Winnik, F. M.; Buschmann, M. D. *Carbohydr. Polym.* **2010**, *80*, 1137–1146.
(49) Lavertu, M.; Xia, Z.; Serreqi, A. N.; Berrada, M.; Rodrigues, A.; Wang, D.; Buschmann, M. D.; Gupta, A. *J. Pharm. Biomed. Anal.* **2003**, *32*, 1149–1158.

analyzed according to Andersson et al.[50] by constructing the Debye plot using the Berry[51] method. The extrapolation to zero scattering angle yields the slope from which the radius of gyration was calculated. The DLS measures the autocorrelated function leading to the diffusion coefficient from which the hydrodynamic radius was calculated using the Stokes−Einstein equation. Each fractogram presented is representative of triplicate samples.

Ultracentrifugation and Orange II Colorimetric Assay. The free chitosan content in DNA/chitosan dispersions was determined by subjecting the samples to ultracentrifugation and measuring the concentration of chitosan in the supernatant by the Orange II depletion method.[52] Samples (600 μL) were ultracentrifuged at 65 000 rpm for 30 min (Beckman Coulter, Optima MAX-E, TLA-110 fixed rotor; Fullerton, CA, USA). The supernatant (100 μL) was collected and diluted 10−20-fold with 50 mM acetic acid/sodium acetate buffer at pH 4.0 such that the concentration of Orange II was always in excess compared to the amino groups of the chitosan to be assayed. A solution of Orange II in the acetic acid/sodium acetate buffer (100 μL, 1 mM) was added to the diluted supernatant (1 mL) and incubated for 45 min. The resulting suspension was centrifuged at 20000*g* for 30 min using a Thermo IEC Micromax microcentrifuge (Needham Heights, MA, USA) to separate the chitosan/Orange II particles and recover the supernatant containing the unbound dye. The absorbance at 484 nm of the supernatant was then measured. The free chitosan content in DNA/chitosan dispersions was calculated from calibration curves obtained by carrying out the same protocol with solutions of chitosan of identical molar mass and DDA. The reported values are the average (±standard deviation) of triplicates.

ζ Potential. The complexes were diluted 4 times in the running buffer prior to analysis with a Malvern Zetasizer Nano ZS (Worcestershire, U.K.). The ζ potential of the complexes was calculated from the electrophoretic mobility values using the Smoluchowski equation.

RESULTS AND DISCUSSION

AF4 operating conditions optimized previously for the fractionation of DNA/chitosan dispersions were used in this study without further modifications.[7] They allow a 87−92% mass recovery of chitosan injected alone and a mass recovery of 95% for DNA/chitosan complexes. The elution of the separated species was monitored by UV−vis, MALS, and DLS detectors in series. The accuracy of the particle hydrodynamic sizes measured by online DLS was confirmed by batch DLS measurements of the same samples prior to AF4 separation and by SEM observations of collected fractions at different elution times.[7] Monitoring the absorbance at 260 nm allowed the detection of DNA in the complexes. A rhodamine B labeled chitosan (Ch-rho) was used to quantify by UV−vis detection the amount of eluted free Ch-rho (λ = 556 nm).

Effect of the Concentration of the DNA Solution Mixed with Rhodamine B Labeled Chitosan Solution on the Size of the Complexes. Previous studies using batch-mode DLS measurements have shown that the hydrodynamic radius of DNA/chitosan complexes increases with the concentration of DNA in the solution used to prepare the nanoparticles.[2,44] To assess the ability of the AF4/UV−vis/MALS+DLS system to detect this change in particle size, we prepared two batches of DNA/rhodamine B labeled chitosan complexes, starting from solutions having a DNA concentration of 82 or 164 μg/mL. The N/P ratio was set at 5 by adjusting the concentration of the Ch-rho solution prior to mixing with DNA. The dispersion obtained with the highest DNA concentration was diluted twice with deionized water prior to injection, so that the injected amount of DNA was the same, allowing direct comparison of the elution profiles. The AF4/UV fractograms are shown in Figure 1A, together with the fractogram of a solution of Ch-rho used as control (corresponding to a DNA concentration of 0 μg/mL). The latter resulted in a single elution band between 1 and 9 min. The intensity of this band is lower in the fractograms of the DNA/Ch-rho dispersions as a result of the complexation, but its elution time is the same.

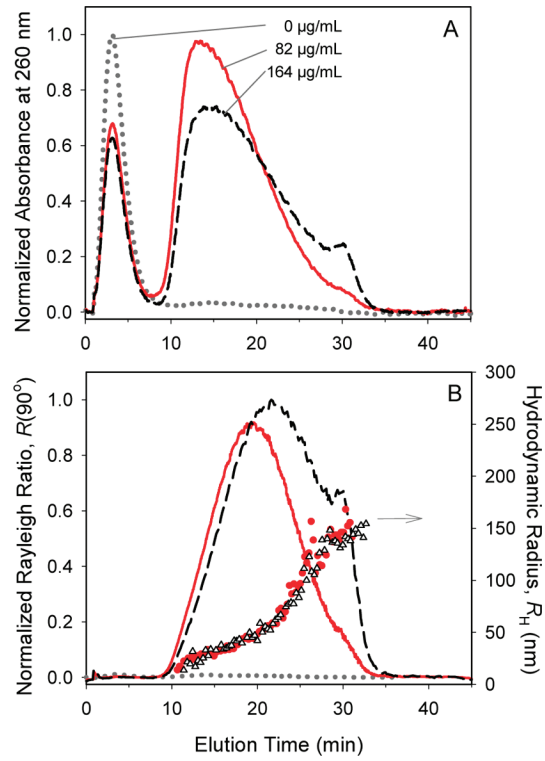

Figure 1. AF4/UV/MALS+DLS fractograms of dispersions of DNA/Ch-rho complexes prepared from mixtures of DNA and Ch-rho (80% DDA, 42 kDa) at initial DNA concentrations of 82 μg/mL (red, —, ●) and 164 μg/mL (black, --, Δ) (N/P = 5). Also shown are the signals upon injection of a Ch-rho solution without DNA as the control sample, corresponding to a DNA concentration of 0 μg/mL (gray, ···): (A) UV detection at 260 nm; (B) Rayleigh ratio at 90° (lines) and hydrodynamic radius (symbols).

The UV fractogram of each DNA/Ch-rho dispersion presents a band at longer elution times, between 9 and 34 min, attributed to the elution of the DNA/Ch-rho nanoparticles, as confirmed by light scattering detection (see below). The complexation between DNA and chitosan is characterized by a high association constant in the range of 10^9−10^{10} M^{-1}.[20] Therefore, in an excess of chitosan, all the DNA is expected to be in the complexed form,

(50) Andersson, M.; Wittgren, B.; Wahlund, K.-G. *Anal. Chem.* **2003**, *75*, 4279–4291.
(51) Berry, G. C. *J. Chem. Phys.* **1966**, *44*, 4550–4564.
(52) Drogoz, A.; David, L.; Rochas, C.; Domard, A.; Delair, T. *Langmuir* **2007**, *23*, 10950–10958.

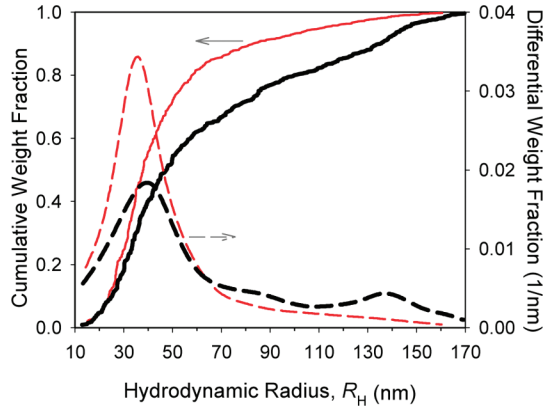

Figure 2. Cumulative (full lines) and differential (dashed lines) weight fractions of AF4/UV/DLS fractionated DNA/Ch-rho (80% DDA, 42 kDa) nanoparticles prepared at initial DNA concentrations of 82 (red lines) and 164 μg/mL (black lines) (N/P = 5).

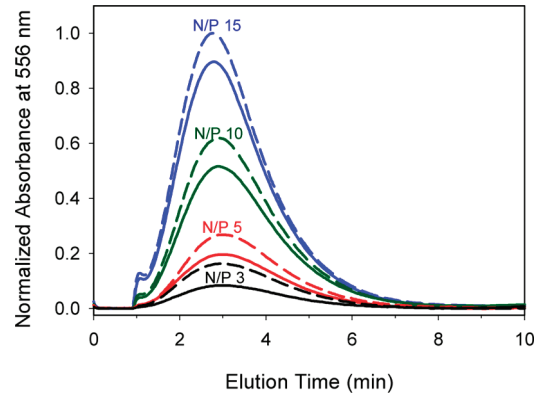

Figure 3. AF4/vis fractograms of free Ch-rho (80% DDA, 42 kDa) before (dashed lines) and after (full lines) complexation with DNA at different N/P ratios monitored by the absorbance at 556 nm. The added DNA concentration was 41 μg/mL.

as confirmed earlier by gel electrophoresis.[53] The nanoparticles eluted in the same time interval, independently of the original DNA concentration, but the intensity and shape of the elution bands were different. The UV profile of the dispersion prepared with the highest DNA concentration features an important shoulder around 30 min. This shoulder, which is barely noticeable in the elution profile of the sample prepared with the less concentrated DNA solution, corresponds to the elution of a small, but significant, population of slightly larger particles. The elution times of the particles and the shape of the UV signals were validated by injecting various dilutions of the same sample (see the Supporting Information, Figure S-1; and in Ma et al.[7]). The integrated area under the curve of the main band as well as the intensity of the shoulder for the various dilutions were proportional to the injected DNA concentration, confirming the absence of overloading effects such as particle−particle interactions.

The elution profiles of the DNA/Ch-rho complexes monitored by MALS and DLS detectors are presented in Figure 1B. The elution band (9−34 min) corresponds to the complexes which have hydrodynamic radii (R_H) ranging from 15 to 160 nm, as calculated from the DLS signals. Smaller particles elute prior to larger ones because they have a higher diffusion coefficient and, consequently, are less retained by the cross-flow in the AF4 channel. The light scattered by the free Ch-rho (the leftmost peak in Figure 1A) was too weak to be detected at the given range of concentrations. The UV and DLS data were used to obtain the size distributions of the DNA/Ch-rho nanoparticles that are presented in Figure 2 as plots of the cumulative and differential weight fraction distributions of the hydrodynamic radius. Although both preparations produced nanoparticles within the same size ranges, it can be seen that that the lower cumulative curve (black curve) corresponding to the sample prepared with the highest DNA concentration represents a particle population where the weight fraction of large particles is higher than in the other preparation. In batch DLS measurements, large and intensely scattering particles often mask the presence of the smaller particles and can contribute predominantly in intensity-averaged hydrodynamic radii distributions, although in trace amounts as demonstrated in a previous report.[7] In such a case, the data must be interpreted with care in the characterization of polydisperse samples, a situation that is resolved here using AF4/UV−vis/MALS+DLS where a fractionation step takes place *prior* to measurement by DLS. Since the formation of the complexes using an initial DNA concentration of 82 μg/mL yielded in majority smaller particle sizes, this concentration was chosen throughout the study.

Effect of the N/P Ratio of the DNA/Polycation (Ch-rho or Ch) Dispersions on the Free Polycation Content and on the Size of the Complexes. We prepared dispersions with 3 ≤ N/P ≤ 15 by adding Ch-rho (80% DDA, 42 kDa) solutions of increasing concentrations to a DNA solution of constant concentration (82 μg/mL). The amount of free Ch-rho was determined quantitatively on the basis of AF4/vis fractograms monitored at 556 nm. Since neither DNA nor the complexes absorb light at this wavelength, and consequently, do not interfere in the quantification of Ch-rho, these fractograms yield higher accuracy of the free Ch-rho content compared to the traces monitored at 260 nm. Elution profiles are presented in Figure 3 (full lines), together with those of the control samples of Ch-rho without DNA (dashed lines). The free Ch-rho content was determined in each dispersion from the integrated areas under the curves. It increases from 53 to 92%, as the total N/P ratio in the dispersions increases from 3 to 15. The N/P ratio of the DNA/Ch-rho nanoparticles was calculated by subtracting the free Ch-rho concentration from the total Ch-rho concentration (Table 2). It was nearly the same (1.3−1.5) in all samples, even in dispersions containing a large excess of Ch-rho. This finding confirmed that the one-shot fast mixing of DNA with an excess of chitosan generates nanoparticles that cannot be formed by slow titrations of chitosan into DNA, as in isothermal titration microcalorimetry (ITC) where the complexes precipitated once the DNA binding sites were saturated close to charge neutrality.[20] The content of chitosan amino groups in nanoparticles formed by fast mixing is almost 2−3-fold higher than in the case of the slow titration mixing in ITC.

The free chitosan content in DNA/chitosan dispersions was determined also by the depletion method with Orange II, a dye employed previously by Drogoz et al.[52] for the characterization of polyelectrolyte complexes. The dispersions were prepared under identical conditions as the samples subjected to AF4, except that unlabeled chitosan (Ch) was used rather than Ch-rho. The

(53) Strand, S. P.; Danielsen, S.; Christensen, B. E.; Varum, K. M. *Biomacromolecules* **2005**, *6*, 3357–3366.

Table 2. Free Polycation (Ch-rho or Ch) Content in Dispersions of DNA/Polycation Complexes Prepared at Different N/P Ratios

	AF4/vis[b]		ultracentrifuge[d]	
total N/P [a]	free Ch-rho[c] (%)	particles N/P	free Ch[e] (%)	particles N/P
3	53 ± 1	1.4 ± 0.1	61 ± 2	1.2 ± 0.1
5	73 ± 2	1.4 ± 0.1	75 ± 1	1.3 ± 0.1
10	85 ± 1	1.5 ± 0.1	87 ± 1	1.4 ± 0.1
15	92 ± 1	1.3 ± 0.1	92 ± 1	1.3 ± 0.1

[a] With Ch-rho or Ch (80% DDA, 42 kDa) of variable concentrations and added DNA concentration of 41 μg/mL. [b] From absorbance at 556 nm. [c] Percentage of the total Ch-rho concentration. [d] From analysis of the supernatant with Orange II. [e] Percentage of the total Ch concentration. Average values and standard deviations of three independent measurements are shown.

dispersions were subjected to ultracentrifugation to separate the complexes from the medium. The ultracentrifugation step was necessary since the DNA/chitosan complexes also bind to the dye, resulting in an overestimation of the fraction of free chitosan. This technique was preferred over filtration that was suggested by Drogoz et al.,[52] avoiding material build-up and inefficient removal of the DNA/chitosan complexes. The supernatant containing free chitosan was recovered and treated with Orange II dye known to interact with the protonated amino groups of chitosan. The values of free chitosan content determined by the ultracentrifugation method are listed in Table 2, together with the values obtained by AF4/vis analysis. There is an excellent agreement between results of the two methods throughout the series of samples, implying that the low level of rhodamine B labeling of chitosan does not interfere significantly with the complexation between DNA and chitosan, as noted previously on the basis of a comparison of particle size data collected for DNA/Ch and DNA/Ch-rho complexes.[7]

A number of previous studies aimed at determining the fraction of free polycation in DNA/polycation dispersions have been reported. Clamme et al.[5] determined by FCS that dispersions of DNA/PEI complexes with total N/P ratios of 6 and 10 have a constant value of 86% of free PEI (corresponding to an N/P ratio of 0.84 and 1.3 in the nanoparticles, respectively). FCS combined with dual labeling of the components for colocalized signals was used to characterize a dispersion of DNA/chitosan oligomers with a total N/P ratio of 10. The fraction of free chitosan in this sample was determined to be 49%.[23] FCS relies on fitting autocorrelation functions to the contributions of two assumed components, i.e., the free polycation and the complex, each idealized as having one diffusion coefficient. Hence, unlike AF4/UV−vis/MALS+DLS, FCS does not provide a direct measurement of free polycation content. The separation by SEC of dispersions of DNA/PEI complexes with total N/P ratios of 6 and 12 yielded an almost constant particle N/P ratio of 2.5,[1] a value calculated from the concentration of free PEI determined by analysis of collected fractions. The fact that the composition of the DNA/PEI nanoparticles was the same in both dispersions is in agreement with our data. The actual value in that report is higher than the particle N/P ratio determined here for DNA/chitosan dispersions. This discrepancy may reflect differences in the interactions of DNA with the two different polycations. The shorter intercharge spacing on PEI, compared to chitosan, may be a factor contributing to the increased content of amino groups in the DNA/PEI complexes. The discrepancy may also be related to a loss of material adsorbed to the SEC column packing, a problem often encountered with this technique.

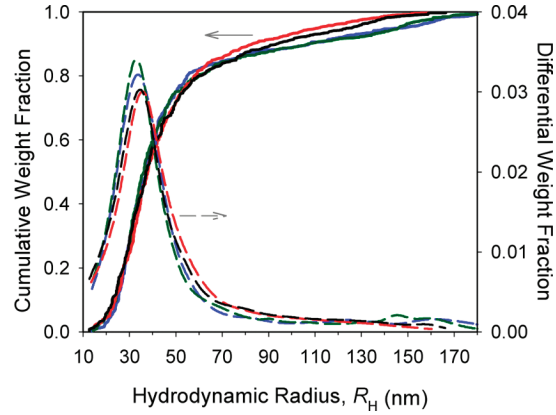

Figure 4. Cumulative (full lines) and differential (dashed lines) weight fractions of AF4/UV/DLS fractionated DNA/Ch-rho (80% DDA, 42 kDa) nanoparticles prepared at N/P ratios of 3 (black), 5 (red), 10 (green), and 15 (blue). The added DNA concentration was 41 μg/mL.

The signals from the DLS and UV−vis detectors can be used also to provide the size distributions of the fractionated particles in dispersions obtained at different mixing N/P ratios (Figure 4). Remarkably, the size distribution was nearly the same in all samples, regardless of the total N/P ratio. This observation, together with the constant composition of the nanoparticles, indicate that the DNA binding sites are saturated under these conditions and that most of the chitosan in excess is free in the aqueous medium. In formulations of DNA/chitosan complexes prepared with N/P ratios up to 20 or 60 in some studies,[2,4,14,15] free chitosan present in high concentration may contribute to the observed enhanced transfection efficiencies. This statement merits further mechanistic analysis, since it is at odds with suggestions made in other studies that such high N/P ratios are necessary for chitosan to fully condense DNA.[14,54]

Effect of the Chitosan Molecular Weight and Degree of Deacetylation on the Characteristics of DNA/Chitosan Dispersions. Previous studies have indicated that the chitosan molecular weight and degree of deacetylation affect the binding affinity of chitosan and DNA, a property related to the ability of the complexes to dissociate for gene expression upon internalization inside the cell nucleus.[4,20,47] The charge density of chitosan can be modulated by its degree of deacetylation, defined as the glucosamine fractional content of the polymer. Dispersions of DNA/Ch-rho of constant total N/P ratio of 5 were prepared with Ch-rho of different DDA and M_n values (see Table 1). The AF4/UV/MALS+DLS fractograms of these complexes are presented in Figure 5A,B. If we consider dispersions prepared with chitosans of comparable molar mass ($M_n \sim 42$ and 35 kDa) but different DDA, we note that their fractograms are very similar, independently of the detection mode (absorbance, Rayleigh ratios at 90° and hydrodynamic radii). The only differences are a more intense peak for the eluted free Ch-rho and a slightly higher absorbance of the complexes with Ch-rho of 72% DDA, compared to the complexes with Ch-rho of 80% DDA. Since

(54) Danielsen, S.; Varum, K. M.; Stokke, B. T. *Biomacromolecules* **2004**, *5*, 928–936.

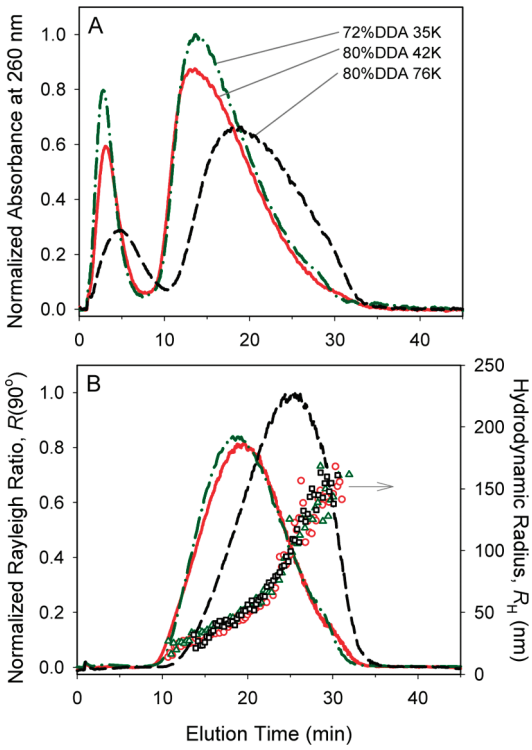

Figure 5. AF4/UV/MALS+DLS fractograms of dispersions of DNA complexed with Ch-rho having different values of DDA and M_n (N/P = 5), showing (A) the absorbance at 260 nm, (B) the Rayleigh ratio at 90° (lines) and the hydrodynamic radius of the nanoparticles with Ch-rho DDA 72% and 35 kDa (Δ), Ch-rho DDA 80% and 42 kDa (○), and Ch-rho DDA 80% and 76 kDa (□). The added DNA concentration was 41 μg/mL.

the number of glucosamines per chain of Ch-rho of 72% DDA is lower than that of Ch-rho of 80% DDA, it was necessary for a constant DNA concentration to add more Ch-rho of 72% than the other one in order to reach the same mixing N/P ratio of 5. Hence, the observed relative intensity of the two bands in the UV traces reflects the higher Ch-rho concentration in the 72% DDA versus 80% DDA dispersions. In addition, the slightly higher level of rhodamine B labeling on the chitosan with a DDA of 72% (Table 1) is a factor which also contributes to these increased intensities observed. The fraction of free Ch-rho calculated from the AF4/vis fractograms was in the order of 71−73% in both samples, resulting in a nanoparticle N/P ratio of about 1.4.

We compare next the elution profiles of dispersions of DNA complexed with Ch-rho samples of identical DDA (80%) but significantly different M_n values (42 and 76 kDa) (Figure 5A,B). The free Ch-rho in the sample obtained with the chitosan of M_n 76 kDa has a longer retention time compared to the sample with a lower molar mass Ch-rho, as expected on the basis of the mechanism of AF4 separation. This trend was also observed in the elution of the nanoparticles: DNA/Ch-rho(76kDa) eluted from 11 to 34 min, whereas DNA/Ch-rho(42kDa) eluted from 8 to 34 min (Figure 5A,B). The highest quartile of the particle size distributions contains larger particles in the sample with the higher molar mass Ch-rho (Figure 6). To further test this observation, we carried out AF4 separations of DNA complexes formed with two additional Ch-rho having a similar DDA (92%)

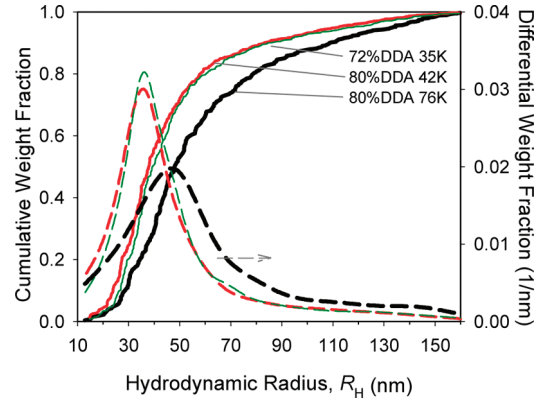

Figure 6. Cumulative (full lines) and differential weight (dashed lines) fraction distributions of the hydrodynamic radius of nanoparticles of DNA complexed with Ch-rho (N/P = 5) having different values of DDA and M_n: 72% DDA and 35 kDa (green lines); 80%DDA and 42 kDa (red lines); and 80%DDA and 76 kDa (black lines). The added DNA concentration was 41 μg/mL.

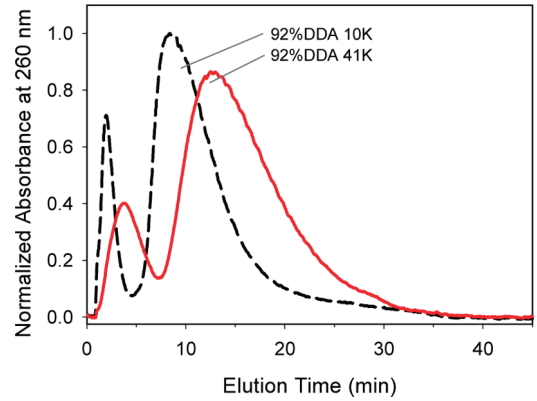

Figure 7. AF4/UV fractograms of dispersions of DNA complexed with Ch-rho having a DDA of 92% but different M_n of 10 and 41 kDa (N/P = 5), monitored by the absorbance at 260 nm. The added DNA concentration was 41 μg/mL.

Table 3. Free Ch-rho Content Determined by AF4/VIS and Other Properties of Dispersions of DNA Complexed with Different Ch-rho (Total N/P = 5)

DDA (%)	M_n (kDa)	free Ch-rho[a] (%)	particles N/P	ζ potential[b] (mV)
72	35	71 ± 2	1.5 ± 0.1	28 ± 1
80	42	73 ± 2	1.4 ± 0.1	29 ± 2
80	76	70 ± 4	1.5 ± 0.2	29 ± 2
92	10	70 ± 2	1.6 ± 0.1	25 ± 2
92	41	73 ± 2	1.4 ± 0.1	29 ± 2

[a] Percentage of the total Ch-rho concentration. [b] By Zetasizer. The added DNA concentration was 41 μg/mL. Average values and standard deviations of three independent measurements are shown.

and different M_n (10 and 41 kDa) (Figure 7). The higher elution times of the nanoparticles formed with the chitosan of 41 kDa compared to the case with the 10 kDa confirm the above observed effect of the chitosan molar mass on the particle size.

The free Ch-rho content in all these samples was determined by monitoring the absorbance at 556 nm (Table 3). It was independent of both the DDA and the M_n of Ch-rho. The calculated N/P value for the nanoparticles composition was once more 1.4−1.6, the range of values recorded in all samples

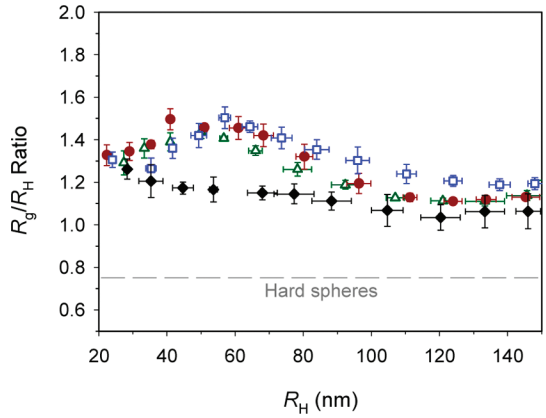

Figure 8. Ratio of the radius of gyration (R_g) to the hydrodynamic radius (R_H) of DNA/Ch-rho complexes (N/P = 5): with Ch-rho DDA 72% and 35 kDa (□); Ch-rho DDA 80% and 42 kDa (●); Ch-rho DDA 80% and 76 kDa (♦); and Ch-rho DDA 92% and 41 kDa (Δ). The added DNA concentration was 41 μg/mL. The broken line represents hard spheres ($R_g/R_H = 0.77$). Average values and standard deviations of three independent measurements are shown.

described in this study (Table 3). We also confirmed that the nanoparticles were always positively charged, in conditions of excess Ch-rho, by carrying out ζ potential measurements of all samples (25−29 mV; Table 3) prior to the AF4 separation.

Conformation of the Complexes: R_g/R_H. Information on the shape of the eluted nanoparticles can be extracted from light scattering data provided by the MALS and DLS detectors. Analysis of the DLS data yields the hydrodynamic radius of the particles. The radius of gyration can be obtained by analysis of the MALS data. The ratio of R_g to R_H provides information on the shape of nanoparticles.[55,56] The values of R_g/R_H derived from AF4/UV−vis/MALS+DLS fractograms of the DNA/Ch-rho nanoparticles prepared with four different Ch-rho (N/P = 5; added DNA concentration of 41 μg/mL) are plotted in Figure 8 as a function of the hydrodynamic radius. R_g/R_H ranged from 1.0 to 1.5, suggesting a conformation similar to that of polymeric stars and clusters rather than hard nondraining spheres (R_g/R_H = 0.78) or rods ($R_g/R_H > 2$).[55,56] This suggests that the nanoparticles adopt a spherical shape with dangling unbound chitosan loops or tails on their surfaces, in agreement with previous reports of SEM imaging of DNA/Ch-rho fractions collected from AF4[7] and of conventional static light scattering analysis of various DNA/polycation dispersions.[22,57] It is interesting to note that the smallest range of R_g/R_H values (1.0−1.3) was recorded for the DNA/Ch-rho complexes formed with the chitosan of highest molecular weight (80% DDA, 76 kDa). It appears that nanoparticles formed with this chitosan had a tendency toward a more compact structure, compared to other samples.[56]

CONCLUSIONS

Five important parameters of DNA/Ch-rho dispersions were obtained simultaneously by AF4/UV−vis/MALS+DLS: the size, the size distribution, the composition, and the conformation of the complexes as well as the free Ch-rho content. The understanding of the influence of physicochemical factors on gene expression relies on the accurate determination of these parameters. Because of the fractionation step, AF4/UV−vis/MALS+DLS was able to detect small changes in the size of complexes obtained by different protocols. The accuracy of the size distribution of polydisperse samples determined by this method exceeds that of batch-mode DLS where the light scattered by large particles dominates the measurement, masking the remaining part of the population, i.e., the smaller particles. The free polycation content was confirmed by ultracentrifugation of the dispersions and subsequent analysis of the recovered supernatant. The composition of the complexes was always about 1.4 in terms of N/P ratio, regardless of the amount of excess chitosan added, molar mass or degree of deacetylation of the chitosan. The information collected in a single analysis by AF4/UV−vis/MALS+DLS of DNA/polycation dispersions promises to be of great help in obtaining a better understanding of structure−activity relationships and in working out strategies to improve the formulations for nonviral gene delivery.

ACKNOWLEDGMENT

This work was supported by the Canadian Institutes of Health Research (CIHR) and by the Natural Sciences and Engineering Research Council of Canada (NSERC). P.L.M. received a doctoral fellowship from the Fonds Québécois de la Recherche sur la Nature et les Technologies.

SUPPORTING INFORMATION AVAILABLE

AF4/UV fractograms at 260 nm of a DNA/Ch-rho dispersion at different dilutions (with Ch-rho 80% DDA and 42 kDa; N/P = 5; initial mixing DNA concentration of 164 μg/mL) and plot of the corresponding integrated peak areas of the nanoparticles versus DNA concentration. This material is available free of charge via the Internet at http://pubs.acs.org.

Received for review March 18, 2010. Accepted October 18, 2010.

AC100711J

(55) Burchard, W. *Adv. Polym. Sci.* **1983**, *48*, 1–124.
(56) Burchard, W. In *Light Scattering: Principles and Development*; Brown, W., Ed.; Oxford University Press: New York, 1996; pp 439−476.
(57) Tan, J. F.; Too, H. P.; Hatton, T. A.; Tam, K. C. *Langmuir* **2006**, *22*, 3744–3750.